Cell Reports, Volume *30*

Supplemental Information

Family-wide Structural and Biophysical Analysis of Binding Interactions among Non-clustered δ-Protocadherins

Oliver J. Harrison, Julia Brasch, Phinikoula S. Katsamba, Goran Ahlsen, Alex J. Noble, Hanbin Dan, Rosemary V. Sampogna, Clinton S. Potter, Bridget Carragher, Barry Honig, and Lawrence Shapiro

Figure S1

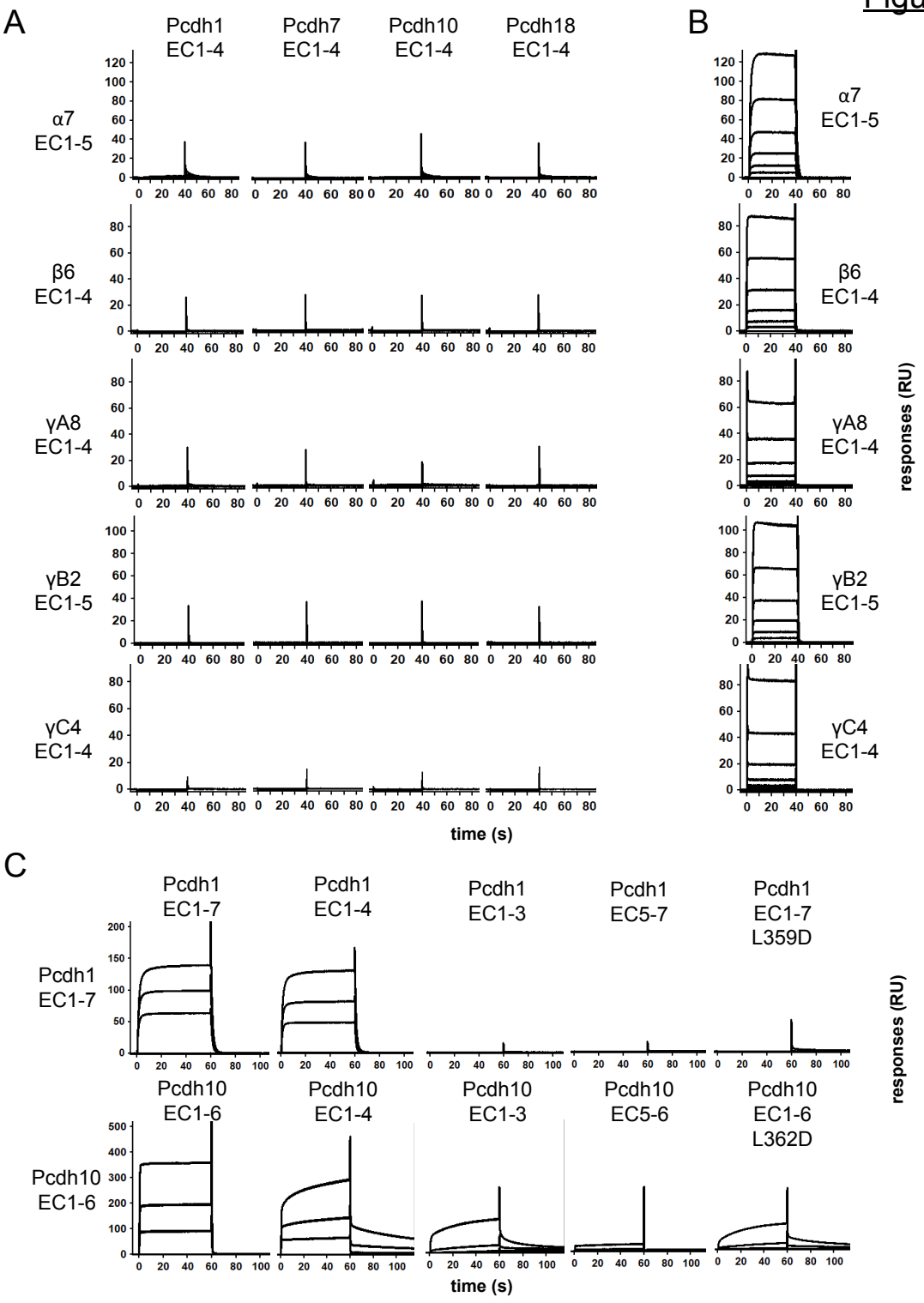

Figure S1: SPR analysis of interactions between δ and clustered protocadherin *trans-binding* fragments and domain-dependence of homophilic δ pcdh homophilic binding, Related to Figure 1.

(A) Assessment of heterophilic binding of EC1-4 fragments of δ pcdhs-1, -7, -10 and -18 to surfaces tethered with clustered pcdh fragments α7 EC1-5, β6 EC1-4, γA8 EC1-4, γB2 EC1-5 and γC4 EC1-4. Each δ protocadherin was tested at three analyte concentrations (27, 9, and 3μM). **(B)** Homophilic binding of the respective clustered pcdhs α7 EC1-5, β6 EC1-4, γA8 EC1-4, γB2 EC1-5 and γC4 over surfaces tethered with biotinylated forms of the same proteins. Each clustered pcdh was tested at six concentrations, 24, 8, 2.67, .89, 0.3 and 0.1 μM. **(C)** Binding of full ectodomains, deletion fragments, and point mutants of pcdh1 (δ1) and pcdh10 (δ2) over the respective full ectodomain surfaces. Analyte concentrations as in panel A.

Figure S2

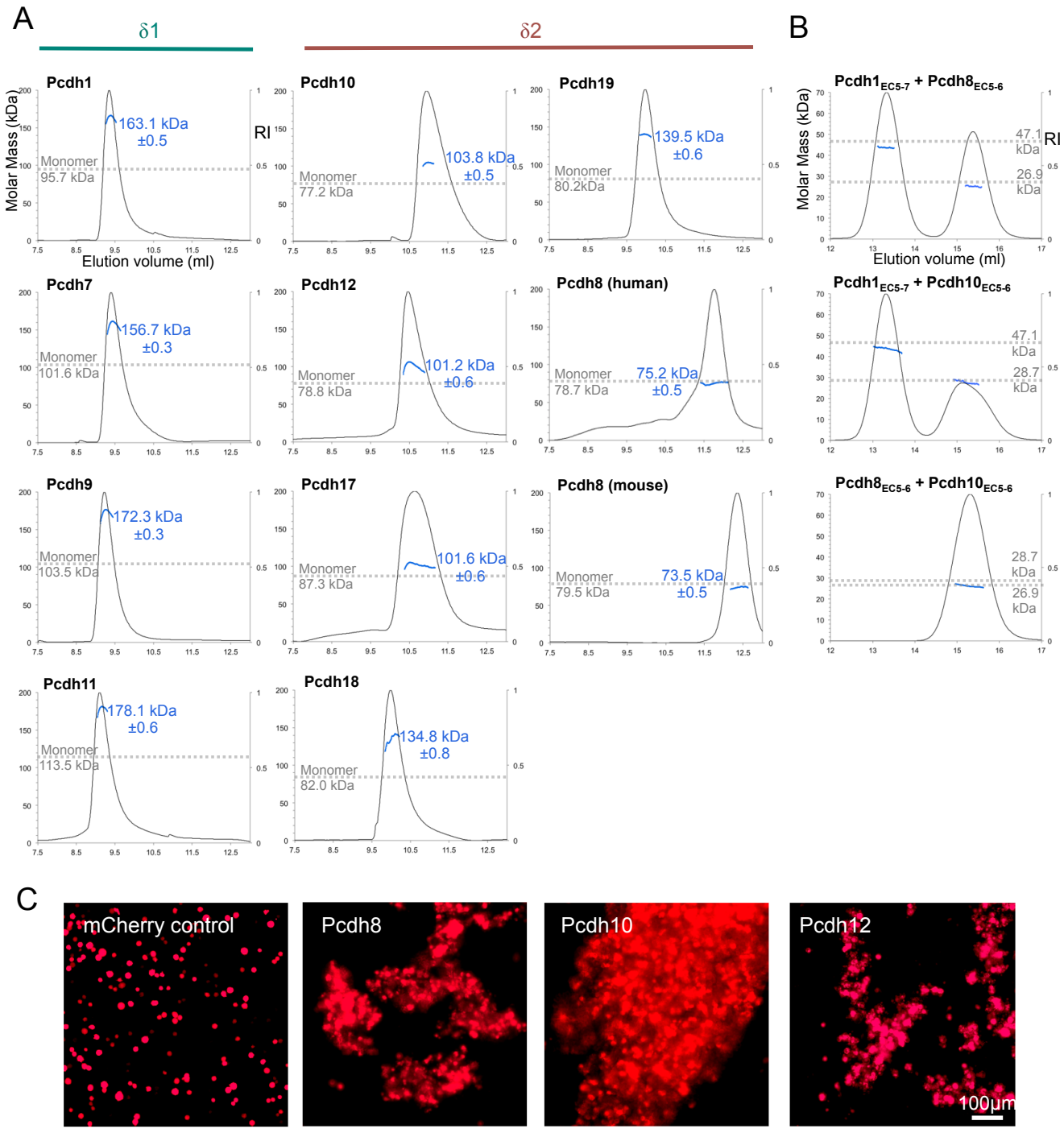

Figure S2: Analysis of δ protocadherin oligomerization state by SEC-MALS and cell aggregation, Related to Table 1.
Purified extracellular regions of δ protocadherins analyzed using size exclusion chromatography (SEC) with in-line multi-angle light scattering (MALS). **(A)** Plots showing protein peaks as refractive index changes (RI, relative scale) against elution volume (ml). Each protocadherin migrated as a single peak. Apparent molecular masses calculated from light scattering analysis are plotted in blue at the peak positions; monomeric molecular masses determined by mass-spectrometry are indicated by a dotted line. All samples were loaded at 24μM concentration. Void volume of the SEC column is ~8ml. **(B)** SEC-MALS analyses of pairwise 1:1 mixtures of membrane-proximal domain fragments of pcdhs-1, -8 and -10 to test potential heterophilic interactions. Loading concentration 100μM for each protein. (**C**) Aggregation of K562 cells transiently transfected with full-length human pcdh-mCherry constructs or mCherry alone, visualized by fluorescence microscopy.

Figure S3

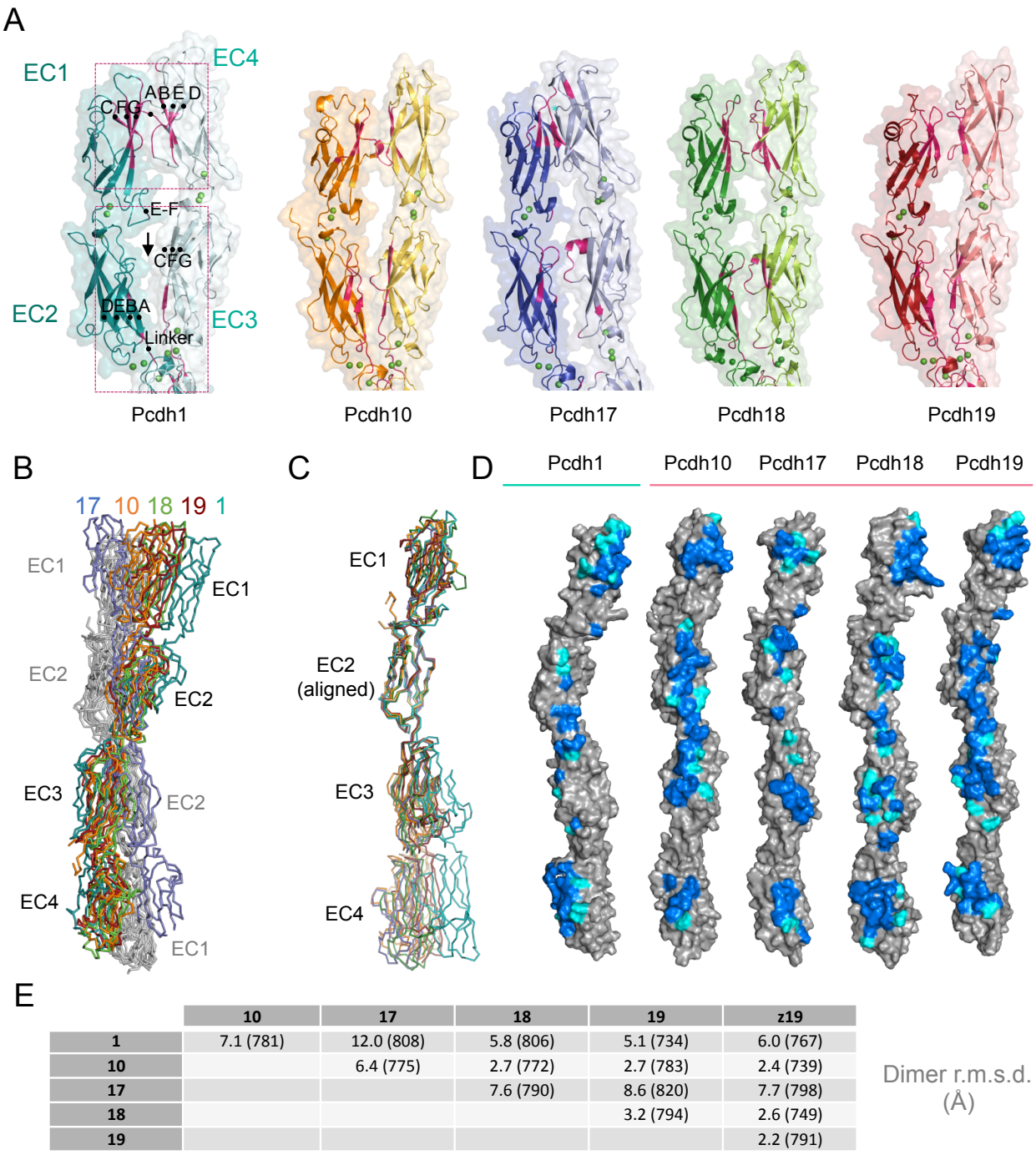

E

	10	17	18	19	z19
1	7.1 (781)	12.0 (808)	5.8 (806)	5.1 (734)	6.0 (767)
10		6.4 (775)	2.7 (772)	2.7 (783)	2.4 (739)
17			7.6 (790)	8.6 (820)	7.7 (798)
18				3.2 (794)	2.6 (749)
19					2.2 (791)

Dimer r.m.s.d. (Å)

Figure S3: Variations in overall *trans* dimer structure between δ protocadherin subtypes, Related to Figures 2 and 3.
(A) *Trans* dimer topologies of pcdhs-1, -10, -17, -18 and -19 (left to right) depicted as ribbons with molecular surfaces. Residues with at least 5% of their accessible surface area buried in the dimer are highlighted in magenta. Dashed boxes delimit EC1:4 and EC2:3 interface regions expanded in Figure 3. Arrow indicates regions of lesser contact in pcdh1. Half of each 2-fold symmetric dimer is shown. **(B)** Cα traces of *trans* dimers superposed over one protomer (background, gray traces) to show differences in orientation of the partner protomer (colored according to legend). **(C)** Individual protomers of the same set of structures as panel (B), superposed over domain EC2 to show differences in interdomain angles. **(D)** Molecular surfaces of single protomers (gray) with *trans* dimer interface residues highlighted in cyan (<5% buried) and blue (>5% buried). **(E)** RMSD values between Cα atoms of superposed whole *trans* dimer structures. Number of aligned Cα atoms indicated in parentheses.

Figure S4

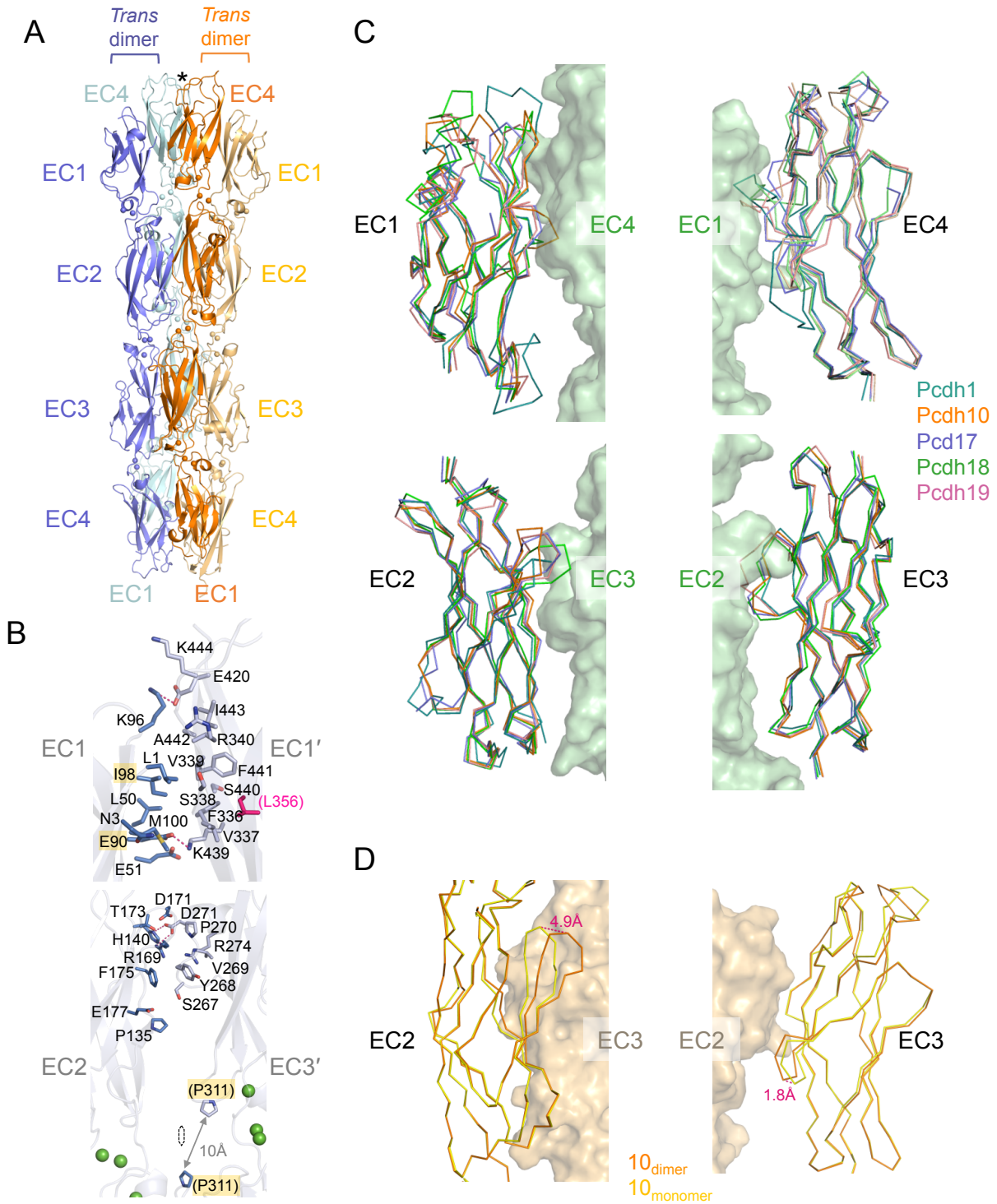

Figure S4: Divergent pcdh17 dimer and variations in interface loop conformations, Related to Figures 2 and 3.
(A) Ribbon view of two putative *trans* dimers of pcdh17 EC1-4 in the crystallographic asymmetric unit. Asterisk indicates a close non-*trans* dimer lattice contact between EC4 domains. Spheres: calcium ions. **(B)** Residue-level view of pcdh17 *trans* dimer interface regions EC1:EC4 (top) and EC2:EC3 (bottom). Side chains of interfacial residues (>5% buried) are shown as sticks; those conserved among δ2 pcdhs are highlighted gold. Leu359 (magenta, equivalent to Leu359 in pcdh10) is solvent exposed. Spheres: calcium ions. **(C)** Carbon α traces of superposed EC domains from *trans* dimer structures of pcdhs -1, -10, -17, -18, and -19. Partner protomer in a representative dimer structure (pcdh10) is shown as a molecular surface (green). **(D)** Superpositions of domains EC2 (left panel) or EC3 (right panel) of monomer and dimer crystal forms of pcdh10, depicted as in panel C. Dashed lines indicate representative shifts.

Figure S5

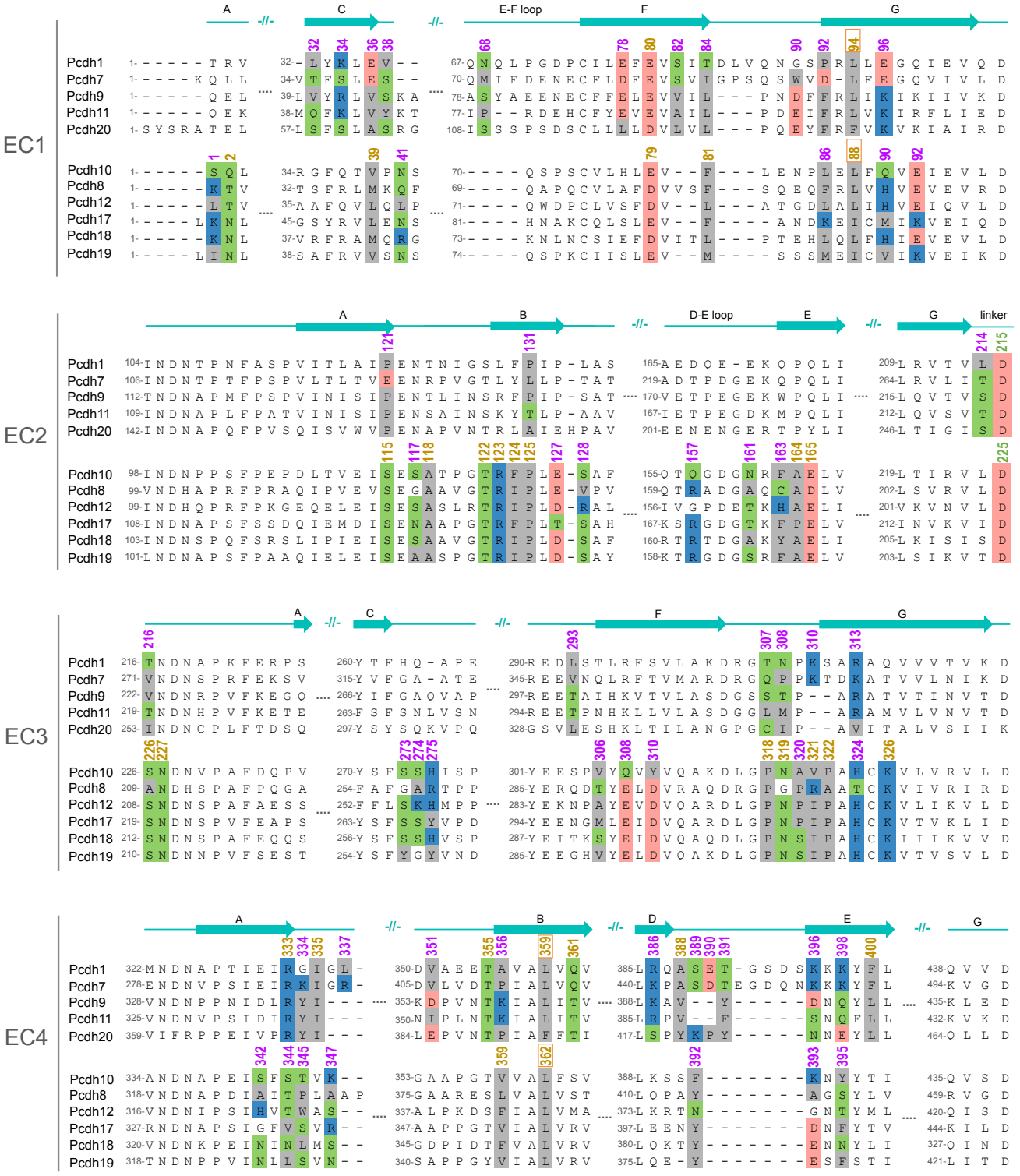

Figure S5: Multiple sequence alignment of human δ protocadherin adhesive domains EC1-4, Related to Figure 3.
Aligned amino acid sequences are separated into δ1 and δ2 subfamilies (top and bottom); secondary structure derives from the pcdh1 structure. Interfacial residue positions from *trans* dimer structures of pcdh1 (δ1) or pcdh10 (δ2) are shaded in all sequences according to amino acid type (gray:nonpolar/aromatic, green:polar, blue:basic, red:acidic, unshaded:glycine) and numbered in gold (conserved in character within subfamily) or purple (non-conserved). Interface numbering refers to pcdh1(top) and pcdh10 (bottom). Interface residues that coordinate Calcium are numbered in green. Pcdh8, which may dimerize weakly, was excluded from δ2 conservation determination. Omitted non-interface regions are indicated by "..." in alignment and by "-//-" in secondary structure.

Figure S6

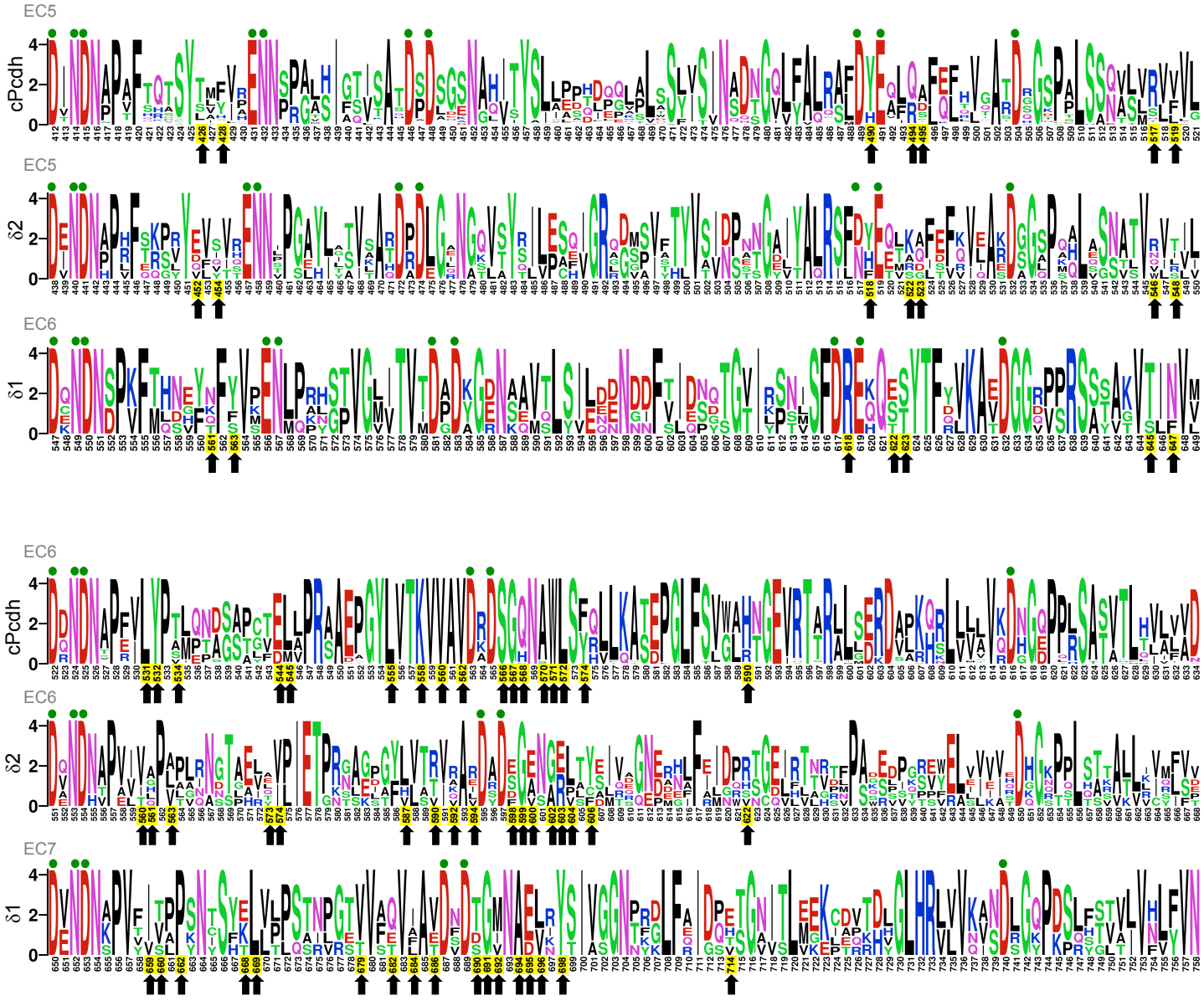

Figure S6: Sequence Logo plot of aligned putative *cis* dimerization regions, Related to Figure 5.
Amino acid sequences of EC5-6 regions of mouse β, γA, and γB clustered protocadherins; EC5-6 regions of human δ2 protocadherins; and EC6-7 regions of human δ1 protocadherins were each aligned to produce Logo plots showing conservation at each residue position. Residue numbering on x axis is based on mouse pcdh γB7 (top plots), human pcdh10 (middle plots), and human pcdh1 (bottom plots); y axis shows estimated information content in bits. Alignments for each domain are displayed separately. Residues whose side chains are buried (>20% ASA) in the *cis* dimer interface of γB7 (PDB:5v5x) and the equivalent positions in δ protocadherins are highlighted with arrows and yellow shading. Calcium co-ordinating residues, which are highly conserved, are marked with green circles above the plots.

Table S1: Crystallographic data collection and refinement statistics, Related to Figures 2 and 5

	Pcdh1 EC1-4 human	Pcdh10 EC1-4 *Monomer form* human	Pcdh10 EC1-4 *Dimer form* human	Pcdh17 EC1-4 human	Pcdh18 EC1-4 human	Pcdh19 EC1-4 human	Pcdh8 EC5-6 human	Pcdh8.1 EC1-6 *Xenopus*		Pcdh10 EC1-6 human	
DATA COLLECTION											
Space group	$P6_122$	$P2_12_12_1$	C2	C2	C2	$P3_221$	$P2_1$	$P2_1$		$P4_12_12$	
***Cell dimensions: a, b, c* (Å)**	148.6, 148.6, 149.9	26.4, 78.9, 238.9	346.6, 73.2, 246.33	214.6, 105.8, 101.4	127.0, 177.0, 71.9	109.0, 109.0, 309.7	41.7, 29.5, 92.4	146.7, 42.4, 167.5		84.1, 84.1, 543.9	
α, β, γ (°)	90, 90, 120	90, 90, 90	90, 132.1, 90	90, 101.0, 90	90, 101.4, 90	90, 90, 120	90, 98.5, 90	90, 110.6, 90		90, 90, 90	
								Spherical[2]	*Ellipsoidal*	*Spherical*[2]	*Ellipsoidal*
Resolution (Å)	40-3.2 (3.42-3.20)[1]	40-2.3 (2.38-2.30)	40-3.6 (3.71-3.60)	40-3.7 (4.0-3.7)	40-2.8 (2.92-2.80)	40-3.5 (3.71-3.5)	40-2.9 (3.07-2.9)	40-2.0 (2.03-2.00)	40-3/3/2 (2.14-2.00)	40-3.3 (3.48-3.30)	40-4.2/4.2/3.3 (3.45-3.30)
R_{merge}	0.12 (1.685)	0.10 (0.89)	0.123 (4.649)	0.211 (0.735)	0.083 (1.24)	0.14 (2.5)	0.13 (0.57)	0.13 (5.28)	0.77 (0.56)	0.139 (2.475)	0.093 (0.52)
R_{meas}	0.12 (1.73)	0.11 (1.00)	0.146 (5.476)	0.248 (0.866)	0.094 (1.41)	0.15 (2.6)	0.16 (0.72)	0.153 (6.03)	0.87 (0.62)	0.145 (2.570)	0.097 (0.54)
R_{pim}	0.028 (0.394)	0.044 (0.44)	0.077 (2.871)	0.128 (0.451)	0.042 (0.64)	0.047 (0.814)	0.08 (0.44)	0.071 (2.87)	0.04 (0.27)	0.040 (0.687)	0.028 (0.15)
CC1/2	1.0 (0.81)	1.0 (0.83)	1.0 (0.29)	1.0 (0.71)	1.0 (0.83)	1.0 (0.72)	0.99 (0.71)	1.00 (0.37)	1.00 (0.88)	1.0 (0.95)	1.00 (0.98)
I/σI	15.9 (2.1)	11.0 (1.6)	5.4 (0.4)	5.4 (1.6)	10.2 (1.4)	9.4 (1.1)	8.2 (1.7)	5.8 (0.3)	12.5 (3.0)	10.7 (1.6)	16.5 (5.8)
Unique reflections	16 684 (2 938)	23 366 (2 283)	52 814 (4 543)	22 957 (4 468)	38 201 (4 506)	27 770 (4 378)	5 168 (803)	128 295 (6 132)	59 482 (2 974)	30 910 (4 386)	20 058 (1003)
Multiplicity	18.3 (19.1)	6.1 (4.7)	3.4 (3.6)	3.5 (3.4)	4.8 (4.6)	9.8 (10.4)	3.3 (2.3)	4.4 (4.1)	4.5 (4.9)	12.9 (13.7)	12.4 (11.9)
Completeness (%)	100.0 (100.0)	99.7 (98.8)	98.2 (98.3)	96.7 (92.1)	97.2 (91.4)	99.9 (99.9)	99.6 (99.1)	97.5 (95.1)	45.1 (12.3)	99.7 (99.5)	64.7 (26.0)
Ellipsoid completeness (%)	n/a	n/a	n/a	n/a	n/a	n/a	n/a	n/a	89.4 (88.8)	n/a	92.1 (97.3)
REFINEMENT											
Resolution (Å)	20-3.2	20-2.3	20-3.6	20-3.7	20-2.8	20-3.5	20-2.9		20-3.0/3.0/2.0[3]		20-4.2/4.2/3.3[3]
Unique reflections	16 561	23 218	50 085	23 284	37 912	27510	5 138		59 447		19771
Molecules per a.s.u.	1	1	5	4	2	3	1		2		1
R_{work}/ R_{free}	0.2255/0.2659	0.1943/0.2333	0.2737/0.2899	0.2508/0.2948	0.2480/0.2692	0.2581/0.2874	0.2250/0.2571		0.253/0.297		0.2410/0.2899
No. atoms											
Protein	3 365	3 282	16 399	12 832	6 742	9 763	1 670		9 847		5006
Ligand/ion	63	57	510	499	262	172	75		184		137
Water	15	105	23	6	50	11	5		138		17
B-factors											
Protein	134.22	57.7	233.3	119.6	110.5	174.0	47.8		69.0		94.3
Ligand/ion	181.13	64.6	245.0	152.9	142.0	229.8	62.3		73.2		117.5
Water	104.53	50.51	225.1	89.3	98.9	130.0	42.0		37.8		36.9
R.m.s deviations											
Bond lengths (Å)	0.0086	0.0130	0.0131	0.0079	0.0160	0.0046	0.0064		0.0057		0.0102
Bond angles (°)	0.552	0.866	0.789	0.818	0.767	0.798	0.811		0.814		0.617
Ramachandran											
Favored (%)	96.8	96.2	96.7	93.5	94.6	94.8	97.3		95.9		95.3
Allowed (%)	3.2	3.8	3.3	6.5	5.4	5.2	2.7		4.1		4.7
Outliers (%)	0	0	0	0	0	0	0		0		0
PDB Accession	6VFP	6VFQ	6VFW	6VFT	6VFR	6VFU	6VFV		6VG1		6VG4

1. Values in parentheses refer to the highest resolution shell
2. Data for pcdh8.1 and pcdh 10 EC1-6 were processed using truncation (Staraniso server) to exclude weak reflections due to diffraction anisotropy; additional values for spherical processing are shown
3. Ellipsoidally truncated data were used in refinement

Table S2: Dimer buried surface areas (BSA), Related to Figure 2

	BSA dimer (Å^2)	Hydrophobic BSA	$BSA_{EC1:4}$	$BSA_{EC2:3}$	$BSA_{EC1\ FG\ loop:EC2}$
Pcdh-1	2986	1859 (62%)[2]	2238 (75%)	652 (22%)	96 (3%)
Pcdh-10	3458 (A:C)[1] 3297 (B:D) 3529 (E:E)	2334 (68%) 2236 (68%) 2307 (65%)	1325 (38%) 1137 (34%) 1479 (42%)	2133 (62%) 2161 (66%) 2050 (58%)	0 (0%) 0 (0%) 0 (0%)
Pcdh-17	2024 (A:D) 2071 (B:C)	1227 (61%) 1288 (62%)	932 (46%) 937 (45%)	1011 (50%) 979 (47%)	81 (4%) 155 (8%)
Pcdh-18	3719	2518 (69%)	2136 (57%)	1534 (42%)	49 (1%)
Pcdh-19	4176 (A:C) 4169 (B:B)	3071 (74%) 2933 (70%)	1994 (48%) 1918 (46%)	2120 (51%) 2252 (54%)	62 (1%) 0 (0%)

1. Values for dimers in crystallographic asymmetric unit are listed separately, indicated by chain IDs
2. Percentage of total dimer BSA

Table S3: Tomography data collection and deposition information, Related to Figure 6.

Tomogram	Tilt range	Nominal Defocus [µm]	Pixel size [Å]	EMDB	Description of biological content
Pcdh1 #1	-39.9-42.9°	-4.02	2.7975	21188	δ1 Pcdh1 EC1-7 ectodomains accumulate at flattened junctional regions between aggregated liposomes. Note apparent midlines and irregular distribution in top views (between vertically stacked liposomes).
Pcdh1 #2	-30.8-52.8°	-4.00	1.83586	21189	
Pcdh1 #3	-46.2-44.0°	-4.00	1.83586	21190	
Pcdh10 #1	-46.0-54.0°	-3.54	1.83586	21191	δ2 Pcdh10 EC1-6 ectodomains accumulate at flattened junctional regions between aggregated liposomes. Note irregular distribution in top views and apparent disorder in junction side views
Pcdh10 #2	-46.0-58.0°	-3.45	1.83586	21192	
Pcdh10 #3	-52.0-50.0°	-3.44	1.83586	21193	